

Behaviour of a pre-defined crack propagating under dynamic tensile loading condition

Rabin Kumar Samal

Indian Institute of Technology, Kharagpur, India

Gangavarapu Teresa Des De Mona

Indian Institute of Technology, Kharagpur, India

Sunita Mishra

Indian Institute of Technology, Kharagpur, India

ABSTRACT: Crack propagating at the rock-tool interface is of paramount importance while designing an excavation process. The present study aims to analyze the behavior of a crack propagating in brittle material like sandstone rock in comparison to ductile material like Aluminum alloy. A three-dimensional finite element model of split Hopkinson pressure bar setup was developed with a pre-cracked dog bone-shaped specimen to understand the behavior of crack using two non-linear strain rate dependent constitutive models, i.e., the Johnson-Cook model and Drucker Prager model. The numerical results were first validated with the experimental ones and then the effect of the crack parallel to the loading direction was studied under dynamic tensile loading conditions. The results show that the peak stress values are more at the center and tip of the crack for aluminum alloy than for the intact aluminum alloy specimens. However, it is completely opposite for sandstone rock.

Keywords: Brittle material, dynamic loading, FE model, pre-crack, SHPB, tensile loading.

1 INTRODUCTION

Construction of tunnels, caverns, development of galleries for extraction of minerals from a mine and various underground structures has always been a challenge due to complex geologic formations of varying hard and soft rock mass. Generally, from the design point of view in order to determine the stability of these subsurface infrastructures and create safer conditions, the overburden load of rock and soil mass is considered. These loads are assumed to be static in nature generating strain rate of 10^{-5} to 10^{-3} per second. But apart from that, there can also be external hazards in form of earthquake, drilling and blasting, terrorist attacks, missile attacks to name a few which are transient in nature. The strain rates caused by earthquakes may vary from 1/s to 100/s and those caused by blasts may vary from 10^2 /s to 10^4 /s. Figure 1 shows the approximate ranges of the expected strain rates achieved through various experimental techniques.

Such high rates of induced strain may have an impact on the rigidity and strength of rocks. Therefore, it is essential to characterize the host rock under both static and dynamic loading conditions for the resilient design of structures embedded in rock strata.

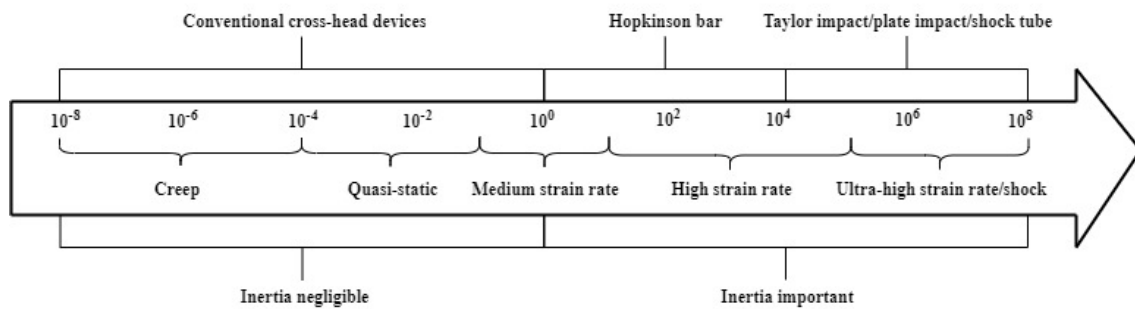


Figure 1. Experimental techniques with varying strain rate regime.

According to Lu et al. (2010), the dynamic compressive test result on different types of rock, i.e., granite, barite, basalt, volcanic tuff, kawazu tuff, red sandstone, Indiana limestone, porphyritic tonalite, oil shale, granodiorite, coal, kidney stone, Tennessee marble, and Akyoshi marble using SHPB device yielding a strain rate of 2000/s. It also revealed that the strain rate has a significant effect on the mechanical behaviour of the rocks as with increasing strain rate the strength of the brittle materials also increases. The resulting data would be useful in precisely analyzing the level of damage that would be caused to any subsurface structure by the action of any external dynamic loads. Studies regarding initiation of fracture, fracture propagation and different types of failure modes in brittle material was first initiated by Griffith (1921). He found that the initiation of the fracture propagation starts at the crack tip and the crack was represented by flat elliptical shape. Griffith (1924) also performed study on brittle materials subjected to biaxial compression and concluded for the expression for tensile failure initiation. The Griffith theory which was originally proposed for the initiation of failure but not for the propagation of failure. Later on, many guidelines, standards, models for testing and designing of underground structures in rock mass under static loading were laid and found in the literature. Moreover researchers have done a detailed study regarding the closure of crack, crack initiation and crack closure point in a brittle type of material like rock (Martin & Christiansson 2009). Thereafter, Lan et al. (2010) have also performed a grain level structural and physical analysis of the rocks using thin sections that helped in providing an input in the discrete element model using UDEC (Itasca 2013). Apart from the work done by Lan et al. (2010), there are many more studies available in the literature which describes about the behaviour of rock and also about the initiation and propagation of crack in rock under static loading condition (Lau & Gorski 1992, Martin & Chandler 1994, Staub & Andersson 2004, Lampinen 2006 and Akesson 2008).

The studies on development of experimental methods for characterization of the mechanical behaviour of materials stating the different modes of failure observed during dynamic loading such as nucleation and coalescence of micro-cracks are of paramount importance for safe designing of underground structures. Moreover, it was found from the literature that the work on dynamic experimental methodologies and the mechanical behaviour of rock materials is neither standardized nor completely understood so far. Paliwal & Ramesh (2006) used high speed imaging technique to analyze the fracture initiation, propagation and coalescence in Cr-coated transparent polycrystalline aluminum oxynitride material under dynamic loading using SHPB device. They correlated the high-speed images of the specimen under dynamic loading condition in time space domain with measurements of the stresses in the specimen. From the study they analyzed the dynamic progressive failure on the surface of the specimen, however they could not find evidence for the origin of the internal failure in the rock specimen. Paliwal & Ramesh (2008) developed a model for brittle failure under compressive loading with an explicit accounting of micro-crack interactions. A model created by Paliwal and Ramesh depicts the propagation of a wing crack from its initial crack. Zhao & Zhang (2019) performed SHPB tests on Brazilian disc specimen of sandstone rock containing the pre-cracks. From the study, then experimental results showed that the multiple cracks mostly initiate at/or near the pre-crack tips and then propagate in different paths and directions varying by inclination angles leading to the ultimate failure.

The present study has been carried out to analyze the sensitivity of a constitutive model developed for brittle material like rock under dynamic loading condition in comparison to constitutive model

developed for ductile material like Aluminum alloy. A pre crack was introduced in a dog bone specimen used for both ductile and brittle material; and the effect was studied at the crack tip and center.

2 MATERIALS AND METHODS

In the present study, ductile material like aluminum alloy and brittle material like sandstone rock have been considered for the analysis. The experimental stress-strain results for the dynamic tensile loading of the aluminum alloy were obtained from Pothnis et al. (2011). The experimental stress-strain results for the dynamic compressive loading for sandstone rock were obtained from Mishra et al. (2019). The study aims to analyze the difference in behaviour of both ductile and brittle materials with an initial crack when subjected to dynamic tensile loading conditions. Hence for uniformity in analysis, the specimen is considered to be of dog bone shape for both the materials. It is also noted that for the sandstone rock, there have been no dynamic tensile response data available in the literature to the authors knowledge. Hence, for the present study, the dynamic tensile response of sandstone rock was obtained from compressive loading response curve obtained from Mishra et al. (2019). The ratio of compressive strength to tensile strength ratio (σ_c/σ_t) of sedimentary rocks ranges from 8 to 15 (Vutukuri et al. 1974, Brook 1993 and Sheorey 1997). Thereof, a ratio of 10 was utilized for obtaining the dynamic tensile response for the present case. Nevertheless, the process of estimating the stress-strain response under dynamic tensile loading condition of sandstone rock using dynamic compressive loading data is simply an assumption. And there has been no supporting evidence for the compressive to tensile strength ratio under dynamic loading conditions. The numerical simulation for the ductile and brittle specimen is carried out using ABAQUS. The sketch of the specimen designed for the numerical simulation has been shown in Figure 2.

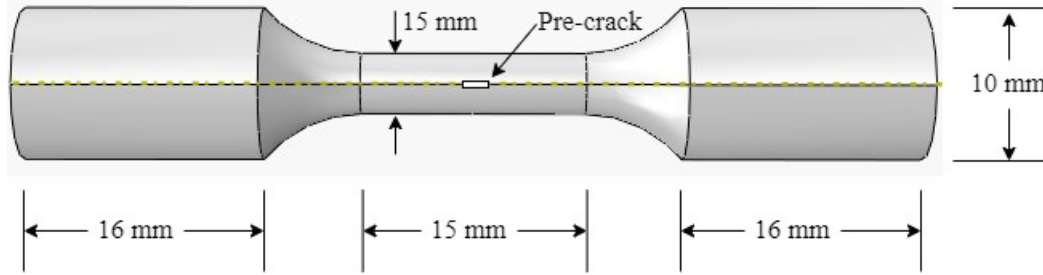


Figure 2. Dog-bone shaped specimen used for both Aluminum alloy and Sandstone rock.

Both uncracked and cracked specimens for ductile and brittle materials have been simulated using Johnson-Cook and Drucker-Prager model, respectively. The equation for Johnson-Cook model is:

$$\sigma = [C_1 + C_2 \varepsilon^n][1 + C_3 \ln \dot{\varepsilon}^*][1 - T^{*m}] \quad (1)$$

where, σ is the von Mises flow stress; C_1 , C_2 , C_3 , n and m are the material constants determined using experimental data; ε is the equivalent plastic strain; $\dot{\varepsilon}^*$ is the dimensionless plastic strain rate; T^* is denoted by $(T_T - T_{\text{room}})/(T_{\text{melt}} - T_{\text{room}})$ where, T_T , T_{melt} and T_{room} are the test temperature, material melt temperature and room temperature, respectively.

The equation for the Drucker-Prager is presented as:

$$F = t - p \tan \beta - d = 0 \quad (2)$$

where,

$$t = \frac{1}{2}q \left[1 + \frac{1}{K} - \left(1 - \frac{1}{K} \right) \left(\frac{r}{q} \right)^3 \right] \quad (3)$$

Here, q is the Mises equivalent stress, r is the third invariant of deviatoric stress, K is the flow stress ratio which is the ratio of yield stress in triaxial tension to yield stress in triaxial compression, p is the equivalent pressure stress, β is the friction angle of the material and d is the cohesion of the material.

3 RESULTS AND DISCUSSION

A three-dimensional numerical model was developed similar to the experimental setup of Mishra et al. (2019) using a finite element software package, ABAQUS. The validation of the numerical model was done with experimental results obtained by Mishra et al. (2019) under dynamic compressive loading condition as shown in Figure 3. The constitutive model used for the validation study was Drucker Prager model and the parameters used are presented in Table 1.

Table 1. Physical properties, elastic properties and various parameters used in the numerical model.

	ρ	E	ν	C_1	C_2	C_3	n	m	T_T
Johnson-Cook model (For Al alloy)	2810	200	0.33	527	676	0.017	0.71	1.61	298
	T_{melt}	T_{room}	$\dot{\epsilon}_0$	-	-	-	-	-	-
Drucker Prager model (For Sandstone)	ρ	E	ν	β	K	ψ	-	-	-
	2339	15.12	0.12	35	0.778	4.38	-	-	-

Note: ρ = Density in kg/m^3 ; E = Young's modulus in GPa; ν = Poisson's ratio; $\dot{\epsilon}_0$ = Reference strain rate per second; β = friction angle of material in degree; ψ = Dilation angle of material in degree.

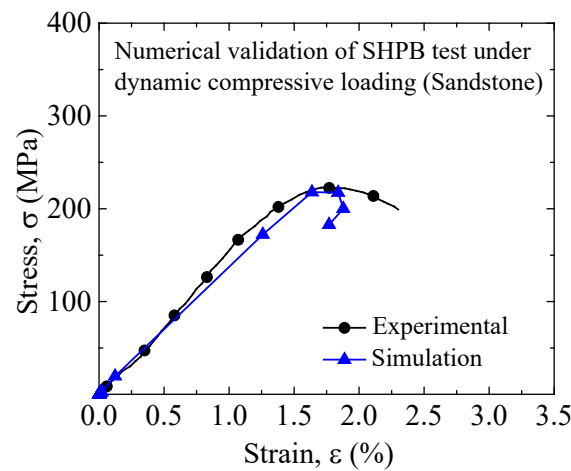


Figure 3. Validation of numerical model with experimental results under dynamic compressive loading condition (Mishra et al. 2019).

Thereafter, a three-dimensional finite element model was developed similar to the experimental setup of Pothnis et al. (2011) and the model was validated with the high strain rate experimental results under dynamic tensile loading rate using Johnson-Cook model (Figure 4a). Now, the Drucker-Prager model parameters validated for sandstone rock using Mishra et al. (2019) was applied to the direct tensile dog bone shaped specimen model developed similar to Pothnis et al. (2011) and the results were observed (Figure 4b). Since the dynamic tensile stress-strain response was derived from experimental results of Mishra et al. (2019), the stress-strain response obtained from direct tensile

dog bone shaped specimen numerical model does not converge with the derived experimental results of sandstone rock. This work shows a scope of dynamic compressive and tensile experimental work to be carried out on sandstone rock.

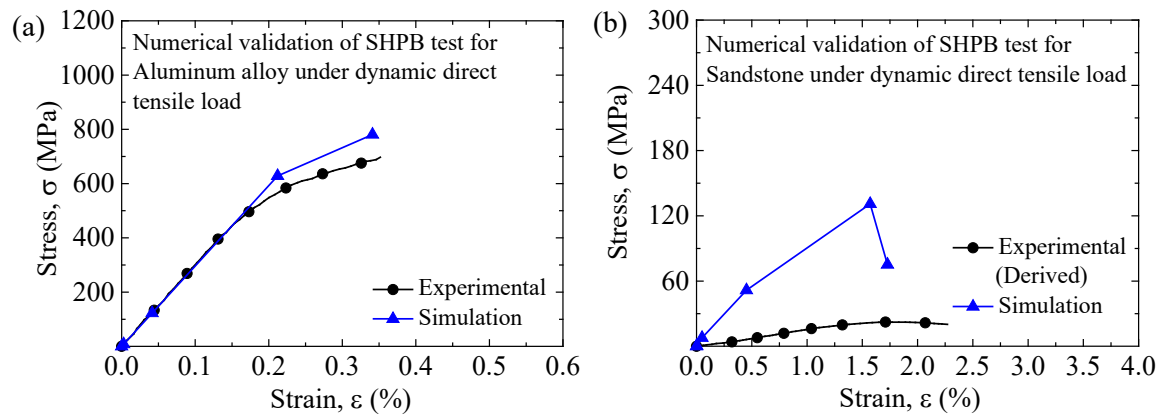


Figure 4. Validation of numerical model with experimental results for (a) Aluminum Alloy (Pothnis et al. 2011) and (b) Sandstone rock under direct tensile loading conditions.

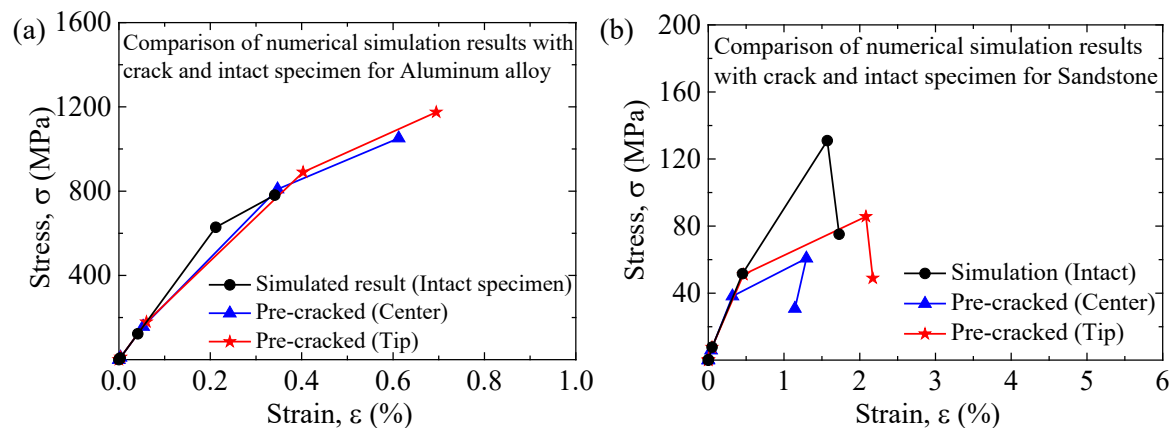


Figure 5. Stress-strain responses of (a) Aluminum alloy and (b) Sandstone rock intact specimen with the crack specimen.

Thereafter, numerical simulations were carried out with pre-cracked specimen (Figure 2) under dynamic tensile loading conditions. The stress-strain response obtained from the center and tip of the crack was plotted with the stress-strain response of intact specimens. It was seen from Figure 5a that for aluminum alloy, the peak stress is 890.31 MPa and 809.22 MPa at the tip and center of the crack, respectively, which is higher than the peak stress value of the simulated intact specimen results, i.e., 628.30 MPa. It is inferred that there may be stress concentration at the tip of the crack than at the center of the crack.

However, for sandstone rock, it is observed that the peak stress values of the intact specimen, i.e., 130.98 MPa is higher than the peak stress values obtained at the tip and center of the crack, i.e., 85.70 MPa and 60.80 MPa, respectively (Figure 5b). This behavior is just the opposite to the behavior observed for aluminum alloy, i.e., ductile material. Due to the brittle nature of sandstone rock, the specimen could not exhibit the strength of an intact specimen.

4 CONCLUSION

It is concluded from the study that there already exists well-established constitutive models for capturing the high strain rate behavior of ductile material. However, a robust database needs to be developed to capture both the dynamic compressive and tensile behavior of rocks. The database will also help in developing the constitutive relations for rock correlating the dynamic compressive loading and dynamic tensile loading parameters.

It is also seen from the results that the peak stress values are more for pre-cracked specimen of Aluminum alloy than for intact specimen. However, it is the opposite for sandstone rock due to its brittle nature.

REFERENCES

- Akesson, U. 2008. *Characterization of micro cracks using core diskings*. SKB Report P-08-103. Stockholm: Swedish Nuclear Fuel and Waste Manage Co.
- Brook, N. 1993. The measurement and estimation of basic rock strength. In *Comprehensive Rock Engineering*, 3, <https://doi.org/10.1016/b978-0-08-042066-0.50009-4>.
- Griffith, A. A. 1921. VI. The phenomena of rupture and flow in solids. *Philosophical Transactions of the Royal Society of London. Series A, Containing Papers of a Mathematical or Physical Character*, 221(582-593), 163-198.
- Griffith, A. 1924. The theory of rupture. In: *First International Congress Applied Mechanics*, 55-63.
- Itasca, U. D. E. C. 2013. 3DEC. Software, Version, 5.
- Lampinen, H. 2006. *Åspö pillar stability experiment. Detailed geological mapping of the pillar blocks*. SKB Report. IPR-05, 24, 67.
- Lau, J. S. O., & Gorski, B. 1992. *Uniaxial and triaxial compression tests on URL rock samples from boreholes 207-045-GC3 and 209-069-PH3*. Canada Centre for Mineral and Energy Technology, Mining Research Laboratories.
- Lu, Y. B., Li, Q. M., & Ma, G. W. 2010. Numerical investigation of the dynamic compressive strength of rocks based on split Hopkinson pressure bar tests. *International Journal of Rock Mechanics and Mining Sciences*, 47(5), 829-838.
- Martin, C. D., & Chandler, N. A. 1994. The progressive fracture of Lac du Bonnet granite. In: *International Journal of Rock Mechanics and Mining Sciences & Geomechanics Abstracts*, 31(6), 643-659.
- Martin, C. D., & Christiansson, R. 2009. Estimating the potential for spalling around a deep nuclear waste repository in crystalline rock. *International Journal of Rock Mechanics and Mining Sciences*, 46(2), 219-228.
- Mishra, S., Chakraborty, T., Basu, D., & Lam, N. 2020. Characterization of sandstone for application in blast analysis of tunnel. *Geotechnical Testing Journal, ASTM*, 43.
- Paliwal, B., Ramesh, K. T., & McCauley, J. W. 2006. Direct observation of the dynamic compressive failure of a transparent polycrystalline ceramic (AlON). *Journal of the American Ceramic Society*, 89(7), 2128-2133.
- Paliwal, B., & Ramesh, K. T. 2008. An interacting micro-crack damage model for failure of brittle materials under compression. *Journal of the Mechanics and Physics of Solids*, 56(3), 896-923.
- Pothnis, J. R., Perla, Y., Arya, H., & Naik, N. K. 2011. High strain rate tensile behavior of aluminum alloy 7075 T651 and IS 2062 mild steel. *Journal of Engineering Materials and Technology*, 133(2).
- Sheorey, P. R. 1997. Empirical rock failure criteria. AA Balkema.
- Staub, I., Andersson, J. C., & Magnor, B. 2004. *Åspö pillar stability experiment. Geology and mechanical properties of the rock in TASQ*. Swedish Nuclear Fuel and Waste Manage Co.
- Vutukuri, V. S., Lama, R. D., & Saluja, S. S. 1974. Handbook on mechanical properties of rocks. *Testing Techniques and Results*, 1, *International Journal of Rock Mechanics and Mining Sciences & Geomechanics Abstracts*, 11(11), A218.
- Zhao, S., & Zhang, Q. 2019. Dynamic crack propagation and fracture behavior of pre-cracked specimens under impact loading by split Hopkinson pressure bar. *Advances in Materials Science and Engineering*.